

University of Arkansas, Fayetteville

ScholarWorks@UARK

Chemical Engineering Undergraduate Honors
Theses

Chemical Engineering

5-2023

Comparing Firocoxib and Meloxicam in the application of Microneedle Patch for Transdermal Drug Delivery

Ruohan Li

University of Arkansas, Fayetteville

Follow this and additional works at: <https://scholarworks.uark.edu/cheguht>



Part of the [Biochemical and Biomolecular Engineering Commons](#), [Biomaterials Commons](#), and the [Other Chemical Engineering Commons](#)

Citation

Li, R. (2023). Comparing Firocoxib and Meloxicam in the application of Microneedle Patch for Transdermal Drug Delivery. *Chemical Engineering Undergraduate Honors Theses* Retrieved from <https://scholarworks.uark.edu/cheguht/190>

This Thesis is brought to you for free and open access by the Chemical Engineering at ScholarWorks@UARK. It has been accepted for inclusion in Chemical Engineering Undergraduate Honors Theses by an authorized administrator of ScholarWorks@UARK. For more information, please contact scholar@uark.edu, uarepos@uark.edu.

Comparing Firocoxib and Meloxicam in the application of Microneedle Patch for Transdermal
Drug Delivery

An Undergraduate Honors College Thesis

in the

Department of Chemical Engineering

College of Engineering

University of Arkansas

Fayetteville, AR

By

Ruohan Li

April 28th 2023

Table of Contents

Abstract

1. Introduction

2. Methods

2.1 Materials

2.2 Solution Preparation

2.3 Microneedle Patch Prep

2.4 Morphological Analysis

2.5 Analysis of Chemical Composition

2.6 Imaging of Micro-needle Patch in Pig Ears

3. Results and Discussion

3.1 Physical Characteristic of Microneedle Patches

3.2 Chemical Composition of Microneedle Patches

3.3 In-vitro Imaging of Microneedle Insertion in Cow's Ear Cadaver Skin

4. Conclusion

5. Acknowledgement

6. References

Abstract

This thesis compares the performance of meloxicam and firocoxib in the aspects of its physical characteristic, chemical compositions, and in-vitro performances for transdermal pain management microneedle patches on farm animals. The microneedle patches are composed of polyvinyl alcohol (PVA), type I collagen (COL), and chitosan (CHI) as base material that carries NSAIDs to achieve therapeutic purposes. Scanning electron microscopy (SEM) was utilized to observe the morphological and physical characteristics of the microneedle patches. Both meloxicam and firocoxib microneedle patches were successfully prepared using the methodology, with organized microneedle distribution and sizing. And Fourier transform infrared spectroscopy (FTIR) confirmed the chemical composition of the PVA-COL-CHI-MEL microneedle patch. The PVA-COL-CHI-MEL microneedle also confirmed its ability to penetrate the skin of pig's ears and dissolve over 24 hours through in-vitro penetration tests. These results revealed the PVA-COL-CHI-MEL microneedle patch's potential to deliver pain-management drugs through transdermal contact.

1. Introduction

Animal welfare refers to the well-being of animals, which includes their physical, emotional, and psychological state. It encompasses a range of factors that affect an animal's quality of life, including the freedom from pain and distress. Pain management is an important aspect of animal welfare, since farm animals often experience pain from various procedures, such as dehorning, castration, docking, and branding [1]. A proper pain management method is necessary to minimize the negative impact of these procedures on animals.

Microneedle transdermal drug delivery has been a pioneering method used to transfer medicine into the animal's body with minimal damage and pain to the body, compared to the traditional injection method of needle delivery. It could also release drugs slowly into the system to maintain longer and more steady effect of the drug. On top of that, due to the longevity of microneedle patches, less doses are required.

Meloxicam is a NSAID-type analgesic, belonging to the oxicam class. Meloxicam reduces pain by inhibiting the production of prostaglandins, which are responsible for pain, inflammation, and fever [2]. Meloxicam also presents promising traits such as a relatively long half-life of 28 hours. Research shows that when oral meloxicam is given at a dose of 1 mg/kg, the highest level of the drug in the bloodstream can be seen between 12 to 24 hours, which is a significant improvement over flunixin meglumine. However, the delivery of meloxicam to animals is currently limited to oral suspension or tablet forms, which are not suitable for prolonged pain relief in livestock [1]. Meloxicam is approved by FDA and commonly prescribed for pain management in domestic pet breeds such as dogs and cats [1].

The NSAIDs perform pain management and reduce inflammation by inhibiting the COX enzymes. The two isoforms of COX enzyme are COX-1 and COX-2, and meloxicam inhibits both COX-1 and COX-2, preferring COX-2 with a ratio of 3.8. Since COX-1 enzyme maintains stability of gastrointestinal mucosal surfaces and renal homeostasis, the inhibition of COX-1 could cause side effects such as gastrointestinal ulceration and bleeding, and renal injury [3]. COX-2 is the enzyme responsible for proteinoids, which triggers pain and inflammation responding to an injury. Inhibiting COX-2 would result in the reduction of pain and inflammation [3]. Therefore, a medication that selectively inhibits COX-2, instead of COX-1, could perform pain management with less gastrointestinal and renal side effects.

Firocoxib is another veterinary prescription NSAID-type analgesic. It also reduces pain by inhibiting the production of prostaglandins. In contrast with meloxicam, firocoxib has a more specific action on the COX-2 enzyme, which is involved in inflammation. The coxib class of nonsteroidal anti-inflammatory drugs was created to offer the therapeutic advantages of COX-2 inhibition, while avoiding the side effects of COX-1 inhibition [4]. Firocoxib has an outstanding selectivity to COX-2 with a ratio of 263-643, compared to meloxicam's selectivity of 3.8. Therefore, animals might experience less gastrointestinal and renal side effects with firocoxib compared to meloxicam [3]. Firocoxib also achieved a long plasma half-life of 47 hours in an equine study, therefore providing sustained pain relief [5].

The medication is vital for the performance of the microneedle patches. However, the structure and chemical composition of the microneedle patches also are deciding factors for steady and safe drug delivery. Though materials such as silicon, metals, and ceramics have been used for microneedle patches in various studies. Polymeric materials have been proven to demonstrate fitting chemical and mechanical properties for microneedle patches [1]. Specifically, chitosan, a cheaper polymer derived from chitin, promises time-release mechanisms in drug delivery. It possesses exceptional qualities that makes it an ideal material for microneedle drug delivery. It exhibits remarkable biocompatibility, non-toxicity, polycationic properties, and biodegradability. In addition, chitosan has been shown to enhance cell adhesion, proliferation, and differentiation, while simultaneously mitigating the risk of infection in fabricating or coating implants [1]. Most importantly, when drugs are embedded in chitosan platforms, the microneedle patch exhibits sustained-release effect due to the swelling and degradation of the chitosan matrix [6]. Since chitosan could be degraded by the body through the kidney, with suitable molecular weight (3-50kDa), chitosan-based micro-patches for humans have been proposed as a proper method for

drug delivery. However, less research has been done on chitosan-based microneedle patches for veterinary uses [1].

Polyvinyl alcohol (PVA) is another polymeric material frequently utilized in microneedle patches for transdermal drug delivery [7]. It is a water-soluble biodegradable polymer which has been applied in dissolving microneedles and often combined with other polymers to strengthen its mechanical properties, reduce material cost, and to realize sustained release of drug [7, 8].

To further improve the microneedle patch's properties, Type I collagen is employed due to its high biodegradability, biocompatibility, and non-toxicity [9]. Additionally, since collagen is the principal protein of extracellular matrix (ECM) and accounts for 75% of the dry weight of skin, a microneedle patch with type I collagen could gain similarity in chemical composition to the ECM at low costs [10].

To enable proper drug delivery, an 8mm x 8mm PDMS mold with 15 x 15 microneedles is utilized to produce dissolving microneedle patches. The microneedles are 600 μm tall and has base length of 300 μm to ensure proper penetration of the skin [1]. Both microneedle patches with composition PVA-COL-CHI-MEL and PVA-COL-CHI-FIR are fabricated using this PDMS mold following strict procedures and methods. The purpose of this thesis is to compare meloxicam and firocoxib based on their performance as microneedle drug delivery patches. Their physical properties, chemical composition, and in-vitro performances are compared using SEM imaging and FTIR.

2. Methods

2.1 Materials

85% deacetylated chitosan (CHI) (molecular weight: 1526.464 g/mol) and 86 to 89% polyvinyl alcohol (PVA) (low molecular weight) were purchased from Alfa Aesar by Thermo Fisher Scientific (cat. no. J64143 & 41238-36 respectively). Collagen Sponges (COL) (Lyophilized type I) derived from bovine tendon was donated by Integra Lifesciences Holdings Corporation, Añasco, PR). For the preparation of PVA-COL-CHI-MEL microneedle patches, Meloxicam (MEL) (pharmaceutical standard, molecular weight: 351.40 g/mol) was purchased from Millipore Sigma (cat. no. PHR1799). The supplier for the polydimethylsiloxane (PDMS; Sylgard 184) molds was Micropoint Technologies Pte, Ltd., Singapore (cat. no. ST-05). The mold, with details shown in Figure 2A, has following dimensions: base size of 8mm x 8mm, needle height of 600 μm , needle base side length of 300 μm , and array size 15 x15, resulting a total of 225 microneedles per patch. 99.8% acetic acid (cat. no. 109088) and phosphate buffered saline (pH 7.2, cat. no. 806544) were from Sigma Aldrich. The ultrapure water system (MilliporeSigma™ Direct-Q™ 3 Tap) produced the ultrapure water, so called Milli-Q® water, at 18 M Ω ·cm from tap water. The ultrapure water was used to dissolve PVC, type I collagen, and chitosan polymer during solution preparation.

2.2. Solution Preparation

Three foundational solutions were needed to prepare the microneedle patches: chitosan (CHI), polyvinyl alcohol (PVA), and collagen (COL) solution.

The chitosan solution was prepared by dissolving chitosan powder in 10% (v/v) of acetic acid in water, resulting in a final concentration of 10% w/v. During this experiment, 1 gram of chitosan was added to 10 mL of acetic acid. The mixture was then placed onto a heating plate at 85°C for

3 hours, to accelerate dissolution. The PVA solution was prepared by dissolving 5 grams of PVA powder in 10 mL of buffer acetate with a pH value of 7.2. The collagen (COL) solution was prepared by dissolving 2 grams of collagen in 10% acetic acid in water (v/v) to a final concentration of 20% collagen (w/v).

2.2.1. Microneedle and Base Solution Preparation

The PVA-COL solution was required for the first layer (microneedles) of microneedle patches, which contains the pain-relief drug. For each patch, the PVA-COL solution contains 31.5 mg PVA solution and 3.5 mg COL solution (ratio 9:1). A second mixture, named PVA-CHI solution, is used for the second layer (base) of the microneedle patch. For each patch, the PVA-CHI solution contained 90 mg of PVA and 10 mg of CHI solution (ratio 9:1).

2.3 Microneedle Patch Prep

The same procedure is repeated for the PVA-COL-CHI-FIR microneedle patch, where meloxicam (MEL) is replaced by firocoxib (FIR).

A PDMS mold measuring 8mm x 8mm was utilized to prepare the microneedle patch. The mold creates microneedle patches with 225 microneedles evenly distributed throughout the patch.

Each needle has a base length of 300 μm and a height of 600 μm , as shown in Fig. 2A.

To begin the preparation process, a mixture of 35 mg of PVA-COL solution and 25 mg of Meloxicam powder was thoroughly mixed for 5 minutes (See Fig. 2 (B) – step 1). Subsequently, the PVA-COL-MEL mixture was spread evenly onto the PDMS mold (See Fig. 2 (B) – step 2). For the third step, the mold was then centrifuged at 4000 RPM for 30 mins, using a Hettich ROTOFIX 32 A Cell Culture Centrifuge from VWR (cat. No. 10813-152). After this process, the initial layer of the microneedle patch was allowed to dry under room temperature for 10 min, thereby creating microneedles consisting of meloxicam (See Fig. 2 (B) – step 4). To generate the

PVA-CHI layer, which is the base layer of the microneedle patch, 5 mL of the PVA-CHI solution was added onto the mold (See Fig. 2 (B) – step 5). The mold with both layers was again centrifuged at 4000 RPM for 5 minutes (See Fig. 2 (B) – step 6). The finished microneedle patch was then dried under room temperature for 24 hours (See Fig. 2 (B) – step 7). Finally, the microneedle patch was gently peeled off the mold (See Fig. 2 (B) – step 8).

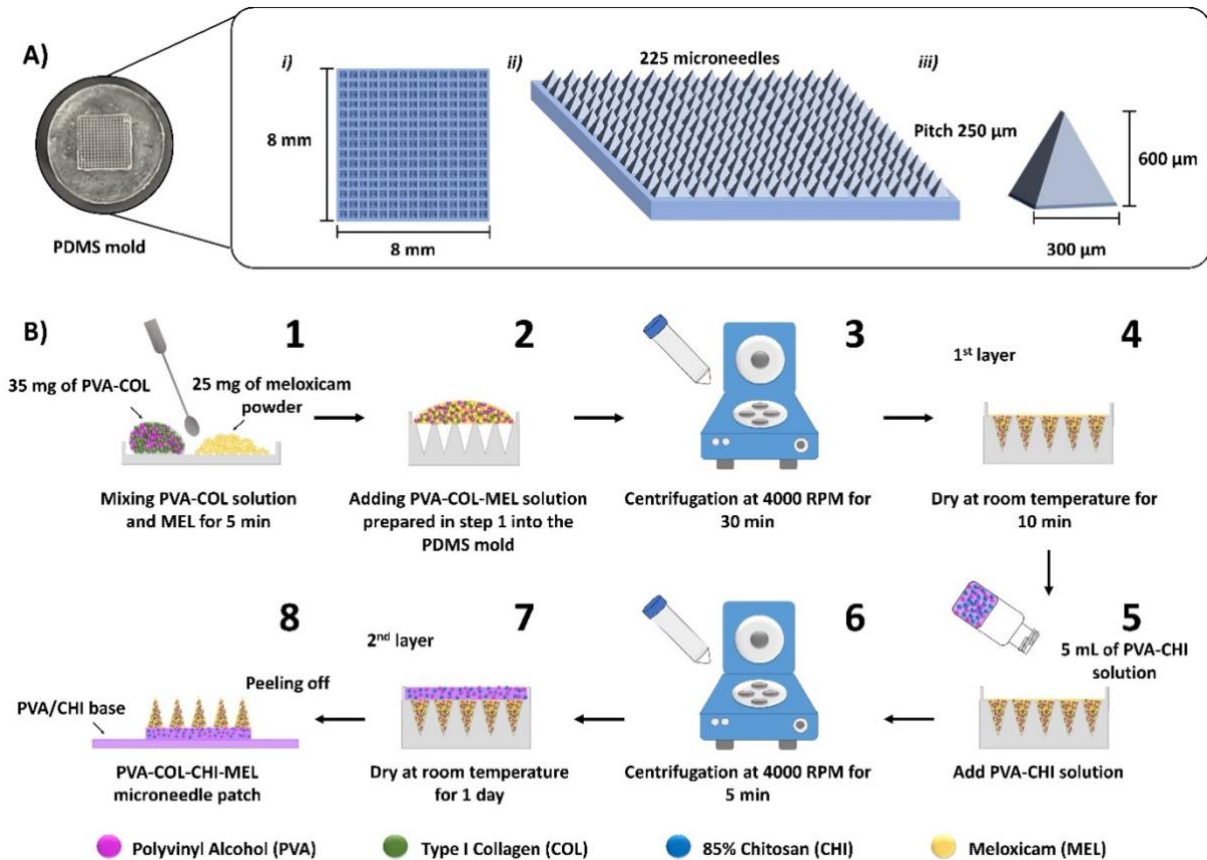


Figure 2. Illustration of chitosan/meloxicam microneedle fabrication process. (A) The details of the PDMS mold and resulting dimensions of microneedles patch (i) PDMS mold has a size of 8mm by 8mm (ii) Side view of the microneedle patch containing 225 microneedles (iii) Each microneedle is 600 μm tall, with a base length of 300 μm, and pitch of 250 μm (B) Step by Step

demonstration of the fabrication process of the dissolving PVA-COL-CHI-MEL microneedle patch

2.4 Morphological Analysis

To examine the form, dimensions, and texture of microneedle patches composed of PVA-COL-CHI, PVA-COL-CHI-MEL, and PVA-COL-CHI-FIR, a TESCAN VEGA3 scanning electron microscope (SEM) was utilized at 5 keV. The same measuring method was applied to the PVA-COL-CHI-FIR.

2.5 Analysis of Chemical Composition

Fourier transform infrared spectroscopy (FTIR) was employed to verify the existence of functional groups in pure CHI, PVA, COL, MEL, and the microneedle patches composed of CHI-COL-PVA-MEL. The samples were subjected to infrared analysis utilizing a PerkinElmer Frontier FTIR with a Diamond ATR holder, over a range of 600-1800 cm^{-1} wavenumbers and 4 scans at 4 cm^{-1} resolution were collected [1].

2.6 In-vitro drug release from the microneedle patch in pig ears

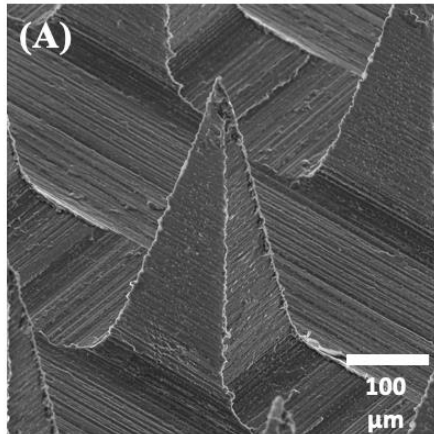
To evaluate the ability of CHI-COL-PVA-MEL microneedle patches to penetrate the skin, frozen pig ears were thawed at room temperature and then prepared by removing all hair from the skin surface. The CHI-COL-PVA-MEL microneedle patches were manually inserted into the cadaver skin of a pig's ear by pressing against their backing layer for 5 second and 24 hours respectively. The skin was allowed to dry at room temperature for 24 hours. To determine the insertion depth, skin images were obtained using a laser microscope 3D & profile measurement (VHX-7000 Series Digital Microscope) from Keyence and a TESCAN VEGA3 scanning electron microscope.

3. Results and Discussion

3.1 Physical Characteristic of Microneedle Patches

SEM imaging was utilized to examine the distribution, morphological characteristics, and topography of the microneedle patches. According to Figure 3, the arrangement and size of the microneedles are consistent between PVA-COL-CHI and PVA-COL-CHI-MEL compositions. The PVA-COL-CHI microneedle has a smooth appearance, closely related to the texture of the PDMS mold. On the other hand, the PVA-COL-CHI-MEL microneedle patch (Fig. 3B and B') has a rough surface texture, potentially due to the meloxicam not completely dissolved in PVA-COL solution.

PVA-COL Microneedle



PVA-COL-CHI-MEL Microneedle

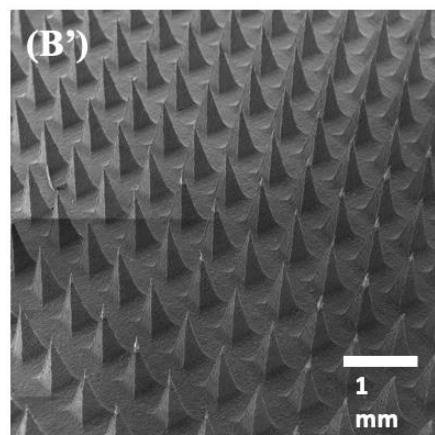
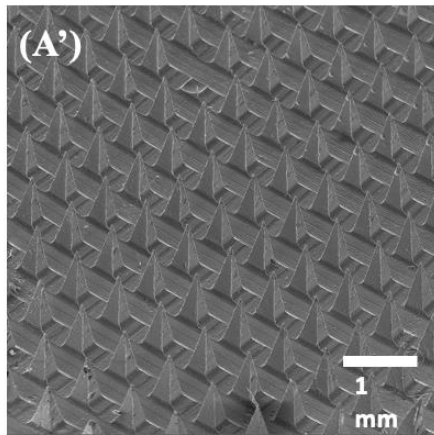
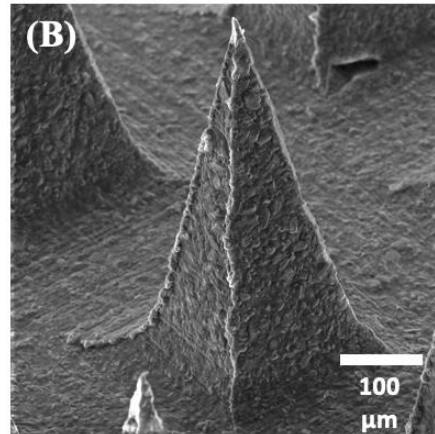


Figure 3. SEM imaging of PVA-COL microneedle and PVA-COL-CHI-MEL microneedle

Similarly, PVA-COL-CHI-FIR microneedle patch also has a rough surface texture, according to Fig. 4A, potentially due to its firocoxib contents. According to Fig. 4A', the distribution of the microneedles is even and organized. Furthermore, each microneedle is formed correctly with needle height discussed in section 2.3. In summary, microneedle patches with the composition PVA-COL-CHI-FIR successfully maintained their shape and topography according to the PDMS mold. Therefore, the microneedle patches containing firocoxib have physical characteristics that are like those containing meloxicam.

PVA-COL-CHI-FIR microneedle

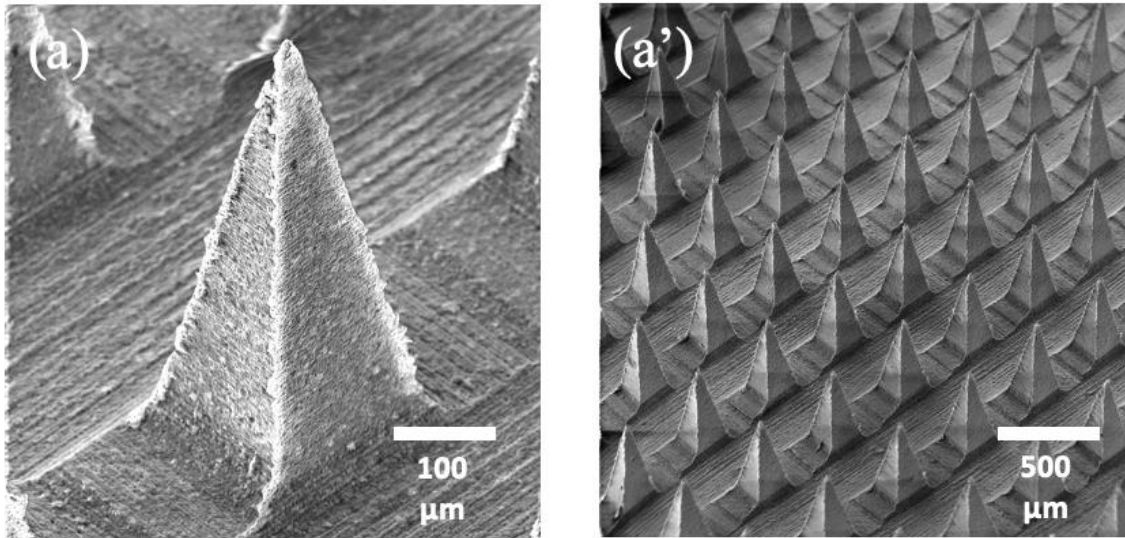


Figure 4. SEM imaging of PVA-COL-CHI-FIR microneedle patch

3.2 Chemical Composition of Microneedle Patches

To demonstrate that all chemical components of the PVA-COL-CHI-MEL microneedle patch are present, Fourier transform infrared spectrum was utilized to map atomic bonds unique to these chemical compounds. The molecular structure of chitosan, meloxicam, collagen, and polyvinyl alcohol are used to compare and analyze the FTIR spectra.

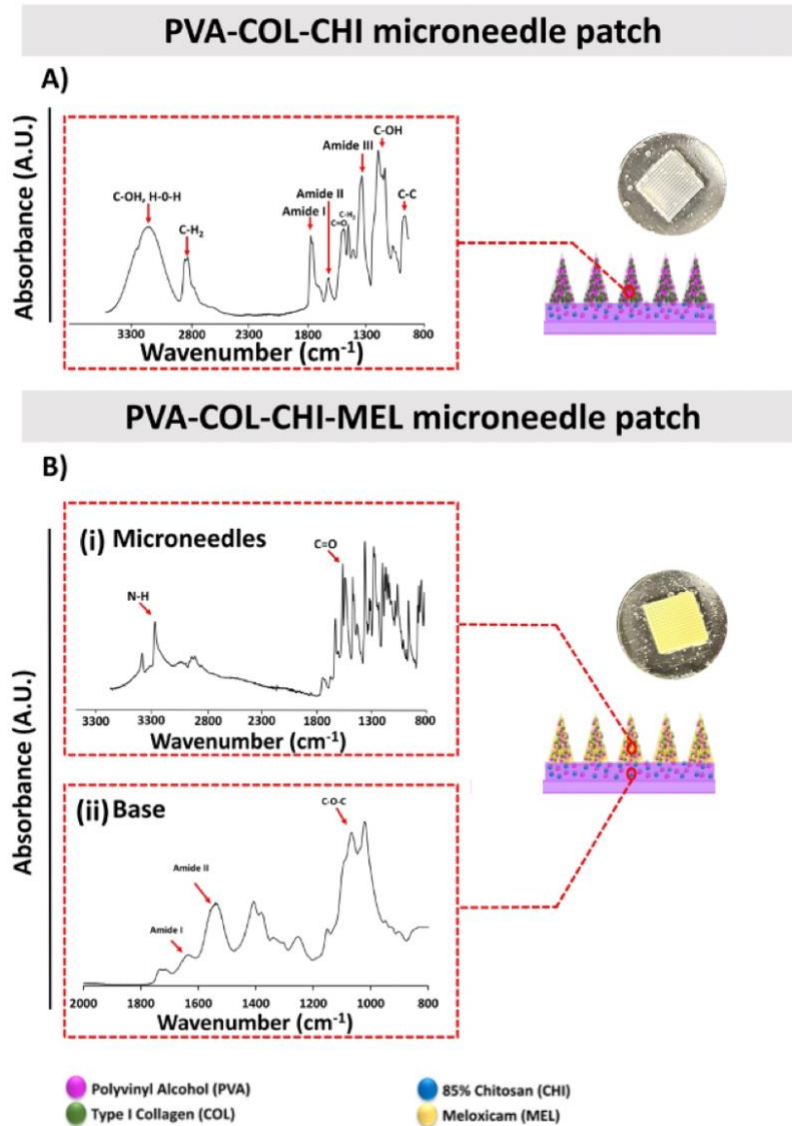


Figure 5. FTIR results of the PVA-COL-CHI and the PVA-COL-CHI-MEL microneedle patches. (A) PVA-COL-CHI microneedle patch (without meloxicam). (B) PVA-COL-CHI-MEL microneedle patch spectrum (i) The microneedle player of the patch, composed of COL-MEL. (ii) The base layer of the patch, composed of PVA-CHI.

Characteristic FTIR absorption peaks of PVA are located at 3249 cm^{-1} (O-H stretching), 2936 cm^{-1} (asymmetric stretching of CH₂), 1643 cm^{-1} (due to water absorption), 1416 cm^{-1} (CH₂ bending), $1150\text{-}1080\text{ cm}^{-1}$ (C-O-C), and 822 cm^{-1} (C-C stretching) [11]. Among the above characteristic FTIR peaks, Fig. 5A indicated the presence of PVA with O-H stretching at 3249 cm^{-1} , CH₂ at 2936 cm^{-1} and the typical PVA (C-C) stretching at 822 cm^{-1} .

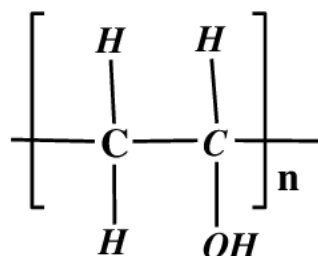


Figure 6. The molecular structure of PVA

Symbolic bonds for Type I collagen include, Amide I with (C=O) at 1660 cm^{-1} , Amide II with (C-N+N-H) at 1554 cm^{-1} , Asymmetric bending with (CH₂) at 1456 cm^{-1} , Amide III vibration from (C-N), (N-H), and (CH₂) at 1236 cm^{-1} , and (C-O) stretching vibration at 1060 cm^{-1} [12]. Among the above peaks, in Fig. 5A, the Amide I, Amide II, Amide II, C=O, and C-H₂ peaks are present in the FTIR spectrum, indicating the presence of type I collagen.

According to the molecular structure of chitosan shown in Figure 7, it is possible to identify its FTIR characteristic absorption peaks at 3435 cm^{-1} (-OH bond), 2922 cm^{-1} (C-H stretch), 1656 cm^{-1} (NH₂ deformation, amide I), 1603 cm^{-1} (N-H, N-acetylated residues, amide II), 1160 cm^{-1} (bridge -O- stretch), 1085 cm^{-1} (C-O stretch, secondary hydroxyl group), and 1030 cm^{-1} (C-O stretch, primary hydroxyl group) according to research [1]. In Fig. 5A, peaks representing C-OH (at $1030\text{ to }1085\text{ cm}^{-1}$), C-H, Amide I, Amide II, and C-OH stretch are present to indicate the chitosan contents in the PVA-COL-CHI microneedle patch.

Chitosan

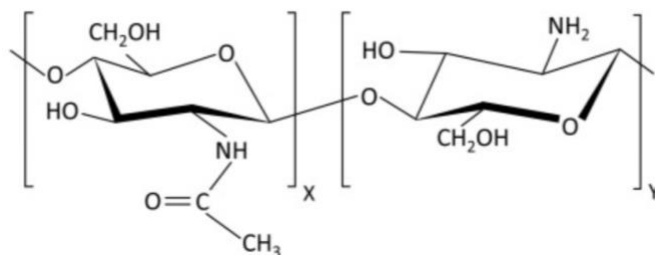


Figure 7. The molecular structure of chitosan [1].

As a result of the above analysis, Fig. 5A confirmed the presence of PVA, COL, and CHI in the PVA-COL-CHI microneedle patch.

In addition, some identifying FTIR peaks for meloxicam are located at 3310 cm^{-1} (amine N-H stretch), 3201 cm^{-1} (O-H stretch), 2850 cm^{-1} (aliphatic C-H stretch), 2905 cm^{-1} (aromatic C-H stretch), 1560 cm^{-1} (C=O stretch), 1340 cm^{-1} (aromatic C=C stretch), and 1190 cm^{-1} (aromatic C=C stretch) according to [1]. Compared to the above information, The FTIR spectrum of CHI-MEL microneedle (Fig. 5B(i)) demonstrates meloxicam presence with N-H amine stretch at 3310 and C=O stretch at 1560 cm^{-1} . Furthermore, the presence of O-H bond at 3435 cm^{-1} and C-H stretch at 2922 cm^{-1} in Fig. 5B(i) also indicated chitosan contents.

Finally, the FTIR spectrum in Fig. 5B(ii) shows Amide I and Amide II peaks, indicating type I collagen presence in the base layer of the microneedle patch. The C-O-C peak at around $1150\text{-}1085\text{ cm}^{-1}$ is evidence for PVA presence. Therefore, confirmed the PVA-COL chemical composition of the microneedle patch base layer.

Due to time constraints, the chemical composition of the PVA-COL-CHI-FIR was not able to be tested using FTIR. Further studies are required to compare results.

3.3 In-vitro imaging of microneedle insertion in cow's ear cadaver skin

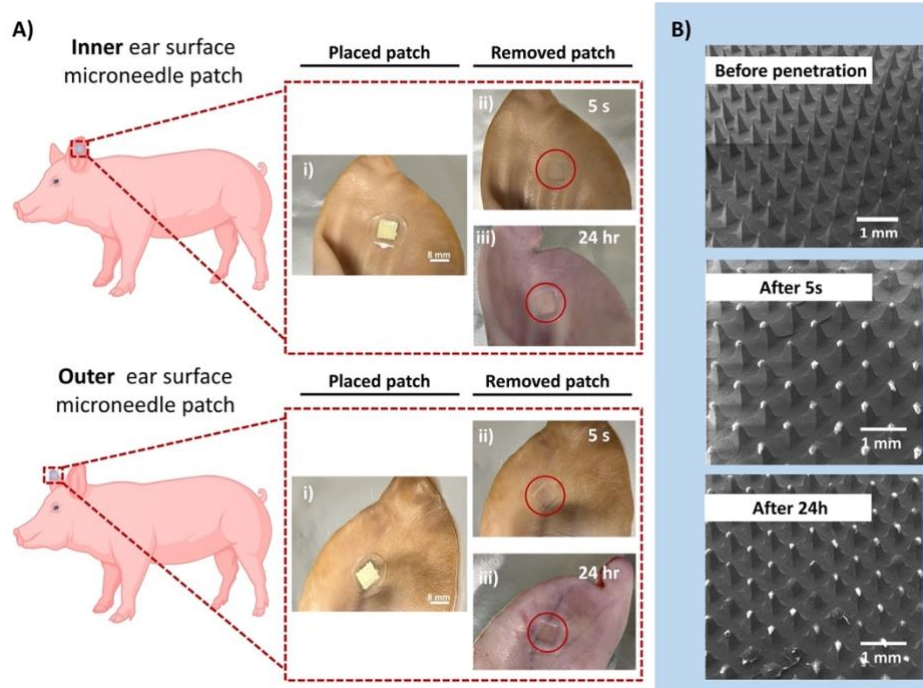


Figure 8. The in-vitro SEM imaging of meloxicam microneedle patches

To examine the skin penetration ability of the microneedle, SEM images were conducted of the SEM imaging of the same microneedle patch (PVA-COL-CHI-Mel) before, 5 seconds after, and 24 hours after penetrating the pig ear. The microneedle patch was prepared according to Section 2.3.

The SEM images in Fig. 8B depict a clear progression: the microneedles have been worn down from the penetration process, indicating successful skin penetration. Furthermore, the second and third images in Fig. 8B demonstrated that the microneedles partially dissolved into the cadaver ear through dermal penetration over 24 hours. These findings suggest that the microneedle patches have the ability to penetrate through the epidermis and dermis layer of the skin, and the needle layer (CHI-MEL) of the patch was able to diffuse into the system over time.

4. Conclusion

Both microneedle patches with composition PVA-COL-CHI-MEL and PVA-COL-CHI-FIR were successfully fabricated according to the methodology of this research. Both microneedle patches have been shown to have organized microneedle distribution and correct needle sizing according to the SEM imaging in Section 3.1. As described in Section 3.2, the chemical composition of the meloxicam microneedle patch was preserved and confirmed through FTIR spectrum. The penetration study of meloxicam microneedle patch (PVA-COL-CHI-MEL) presented successful skin penetration in pig's ear cadaver skin. On top of that, the timed study of the microneedle patch demonstrated its ability to dissolve in the cadaver skin over 24 hours. Due to time constraints, the chemical composition testing and in-vitro microneedle insertion tests were not completed for firocoxib microneedle patches (PVA-COL-CHI-FIR). Therefore, further testing of the firocoxib microneedle patches is necessary to confirm its chemical composition and insertion properties. Future research could include in-vivo testing to compare meloxicam and firocoxib's plasma half-life and their side effects.

5. Acknowledgement

I would like to express my gratitude to my advisor, Dr. Almodóvar of the Ralph E. Martin Department of Chemical Engineering, for his support and guidance throughout my honors thesis project. His willingness to admit me into his lab and provide continuous support have been invaluable to the success of my research. Additionally, I am also immensely grateful to Katherine Miranda, my graduate student mentor, who helped me navigate the challenges of my project with her expertise and dedication. Her coaching and daily support on experiments and thesis writing have been extremely helpful. Without her advice and encouragement, my thesis would not have been possible.

I also extend my appreciation to the Animal Science department for their contribution to this project. They have provided the animal materials, which played a significant role in the achievement of my research goals. Lastly, I would like to acknowledge the US Department of Agriculture for providing funding for this project.

6. References

- [1] Castilla-Casadio, D. A., Carlton, H., Gonzalez-Nino, D., Miranda-Muñoz, K. A., Daneshpour, R., Huitink, D., Prinz, G., Powell, J., Greenlee, L., & Almodovar, J. (2021). Design, characterization, and modeling of a chitosan microneedle patch for transdermal delivery of meloxicam as a pain management strategy for use in cattle. *Materials Science and Engineering: C*, 118, 111544. <https://doi.org/10.1016/j.msec.2020.111544>
- [2] S. E. Papich. "Meloxicam" and "Firocoxib". In: *Saunders Handbook of Veterinary Drugs: Small and Large Animal*. 4th ed. Elsevier, 2016, pp. 543-547 and 324-327.
- [3] Fogle, C., Davis, J., Yechuri, B., Cordle, K., Marshall, J., & Blikslager, A. (2020). Ex vivo COX-1 and COX-2 inhibition in equine blood by phenylbutazone, flunixin meglumine, meloxicam and firocoxib: Informing clinical NSAID selection. *Equine Veterinary Education*, 32(10), 511-516. <https://doi.org/10.1111/eve.13280>
- [4] Meléndez, D. M., Marti, S., Pajor, E. A., Sidhu, P. K., Gellatly, D., Moya, D., Janzen, E. D., Coetzee, J. F., & Schwartzkopf-Genswein, K. S. (2018). Effect of meloxicam and lidocaine administered alone or in combination on indicators of pain and distress during and after knife castration in weaned beef calves. *PLoS One*, 13(11), e0207289. doi: 10.1371/journal.pone.0207289. PMID: 30500846; PMCID: PMC6269141. <https://www.ncbi.nlm.nih.gov/pmc/articles/PMC6269141/>
- [5] Lemonnier, L. C., Thorin, C., Meurice, A., Dubus, A., Touzot-Jourde, G., Couroucé, A., & Leroux, A. A. (2022). Comparison of Flunixin Meglumine, Meloxicam and Ketoprofen on Mild Visceral Post-Operative Pain in Horses. *Animals*, 12(4), 526. <https://doi.org/10.3390/ani12040526>

- [6] Chen, M.-C., Ling, M.-H., Lai, K.-Y., & Pramudityo, E. (2012). Chitosan microneedle patches for sustained transdermal delivery of macromolecules. *Biomacromolecules*, 13(12), 4022-4031. doi: 10.1021/bm301293d.
- [7] Ahmed Saeed Al-Japairai, K., Mahmood, S., Hamed Almurisi, S., Reddy Venugopal, J., Rebhi Hilles, A., Azmana, M., & Raman, S. (2020). Current trends in polymer microneedle for transdermal drug delivery. *International journal of pharmaceutics*, 587, 119673. <https://doi.org/10.1016/j.ijpharm.2020.119673>
- [8] Nguyen, H. X., Dasht Bozorg, B., Kim, Y., Wieber, A., Birk, G., Lubda, D., & Banga, A. K. (2018). Poly (vinyl alcohol) microneedles: Fabrication, characterization, and application for transdermal drug delivery of doxorubicin. *European Journal of Pharmaceutics and Biopharmaceutics*, 129, 230-240. <https://doi.org/10.1016/j.ejpb.2018.05.017>
- [9] Aditya, A., Kim, B., Koyani, R. D., Oropeza, B., Furth, M., Kim, J., & Kim, N. P. (2019). Kinetics of collagen microneedle drug delivery system. *Journal of Drug Delivery Science and Technology*, 52, 743-749. <https://doi.org/10.1016/j.jddst.2019.03.007>
- [10] Makvandi, P., Kirkby, M., Hutton, A. R. J., Shabani, M., Yiu, C. K. Y., Baghbantaraghdari, Z., Jamaledin, R., Carlotti, M., Mazzolai, B., Mattoli, V., & Donnelly, R. F. (2021). Engineering Microneedle Patches for Improved Penetration: Analysis, Skin Models and Factors Affecting Needle Insertion. *Nano-micro letters*, 13(1), 93. <https://doi.org/10.1007/s40820-021-00611-9>
- [11] Deleanu, I., Stoica, A., Stroescu, M., Dobre, L., Dobre, T., Jinga, S., & Tardei, C. (2012). Potassium sorbate release from poly(vinyl alcohol)-bacterial cellulose films. *Chemical Papers*, 66, 138-143. <https://doi.org/10.2478/s11696-011-0068-4>.

[12] Sanden, K. W., Kohler, A., Afseth, N. K., Böcker, U., Rønning, S. B., Liland, K. H., & Pedersen, M. E. (2019). The use of Fourier-transform infrared spectroscopy to characterize connective tissue components in skeletal muscle of Atlantic cod (*Gadus morhua* L.). *Journal of Biophotonics*, 12(8), e201800436. <https://doi.org/10.1002/jbio.201800436>.

Appendix

Extra sources I found that could be useful, but not officially included in the paper:

[a] Kivett, L., Taintor, J., & Wright, J. (2013). Evaluation of the safety of a combination of oral administration of phenylbutazone and firocoxib in horses. *Journal of Veterinary Pharmacology and Therapeutics*, 37(5), 512-516. <https://doi.org/10.1111/jvp.12097>

[b] Lemonnier, L. C., Thorin, C., Meurice, A., Dubus, A., Touzot-Jourde, G., Couroucé, A., & Leroux, A. A. (2022). Comparison of Flunixin Meglumine, Meloxicam and Ketoprofen on Mild Visceral Post-Operative Pain in Horses. *Animals: an open access journal from MDPI*, 12(4), 526. <https://doi.org/10.3390/ani12040526>

[c] Kivett, L., Taintor, J., & Wright, J. (2014). Evaluation of the safety of a combination of oral administration of phenylbutazone and firocoxib in horses. *Journal of veterinary pharmacology and therapeutics*, 37(4), 413–416. <https://doi.org/10.1111/jvp.12097>